Progress In Electromagnetics Research Letters, Vol. 55, 31–38, 2015

Dual-Band Bandpass Filters Using a Novel Quad-Mode Stub-Loaded Ring Resonator

Lei Lin*, Pan-Pan Xu, Jin-Lin Liu, Bian Wu, Tao Su, and Chang-Hong Liang

Abstract—This paper presents two dual-band bandpass filters with controllable passband frequencies and bandwidths. The filters are realized utilizing a novel quad-mode stub-loaded ring resonator. All the four mode equivalent circuits of the resonator are quarter-wavelength resonators, and their fundamental resonance frequencies are used to form the passbands. So the designed filters have a compact circuit size and relatively wide upper stopband. For validation, two experimental filters operating at 1.5/2.4 GHz and 1.5/3.5 GHz are designed. In the design of the second filter, hook-shape feed-lines and source-load coupling are applied to generate more transmission zeros, which greatly improve the selectivity of the filter. Finally, the filters are fabricated, and measured. The measured results have good agreement with the simulated ones.

1. INTRODUCTION

Multi-band microwave components are often required in modern wireless communication systems, and dual-band bandpass filter (BPF) becomes a good candidate. A variety of configurations were proposed to design dual-band BPFs. In [1], two E-shape resonators were cascaded to construct a dual-band BPF. In [2–8], various multiple mode stub-loaded resonators (SLRs) and stepped impedance resonators (SIRs) were proposed to implement dual-band BPFs. Meandering SIRs were utilized in [9] to design a dual-band BPF with narrow passbands. In [10], two multi-mode resonators were connected together by a grounded via to implement a dual-band BPF with three transmission poles in each passband. All the dual-band BPFs presented in the above-mentioned literatures were designed using two or more resonators, and the circuit sizes are relatively large. For miniaturization, a variety of multi-layer structures or multiple mode resonators were proposed, and using the proposed structure, or the single multi-mode resonators, compact multi-band BPFs were designed [11, 12]. Recently, many reports have been published about dual-mode dual-band BPFs [13–17], in which the first harmonic even- and odd-mode frequencies of the resonator are utilized to form the second passband, thus leading to both passbands dependent on each other which is undesirable in the filter design. A 2-order dual-band BPF using a single multi-mode circular ring resonator was proposed in [18]. In order to realize two controllable passbands center frequencies, periodic open-stubs are loaded, which leads to increased radiation loss and deterioration of in-band performance. In [19], a dual-mode split microstrip resonator was presented and its even- and odd-modes can be varied independently in a wide range and the two lower resonant frequencies maybe arbitrary close to each other. Using the split microstrip resonator, the author implemented a variety of compact high performance filters and other frequency selective devices [20]. In [21], a microstrip square ring resonator with open-circuited stubs loaded was proposed. The loaded stubs excite and slit two first-order degenerate modes, and a dual-band BPF was design based on it.

In this paper, a novel quad-mode stub-loaded ring resonator is proposed and its resonance characteristics are analyzed theoretically using the even-odd-mode method. Through the analysis,

Received 13 July 2015, Accepted 12 August 2015, Scheduled 15 August 2015

* Corresponding author: Lei Lin (yeslinlei@gmail.com).

The authors are with National Key Laboratory of Antennas and Microwave Technology, Xidian University, Xi'an 710071, China.

all the equivalent circuits of the four modes are quarter-wavelength resonators. Based on the proposed resonator, two compact dual-band BPFs with controllable passband frequencies and bandwidths are implemented, these exhibit very good performance. In the design of the second filter, the properly designed feedlines generate more transmission zeros (TZs), which greatly improve the selectivity and the isolation level between passbands of the filter. The measured results of the fabricated filter are in good agreement with the simulated ones.

2. ANALYSIS OF THE PROPOSED QUAD-MODE RING RESONATOR

The structure of the proposed quad-mode resonator is depicted in Figure 1. P-P' indicates the symmetry plane of the resonator. Due to its symmetry, the resonance characteristics are analyzed using the even-odd-mode method. Under even-mode excitation, the symmetry plane P-P' can be considered as a magnetic wall, the short-ended stubs are bisected and the widths are half what they were. The even-mode equivalent circuit is shown in Figure 2(a). Under odd-mode excitation, the symmetry plane P-P' behaves as an electric wall, and the short-ended stubs are ignored. The odd-mode equivalent circuit is shown in Figure 2(b).

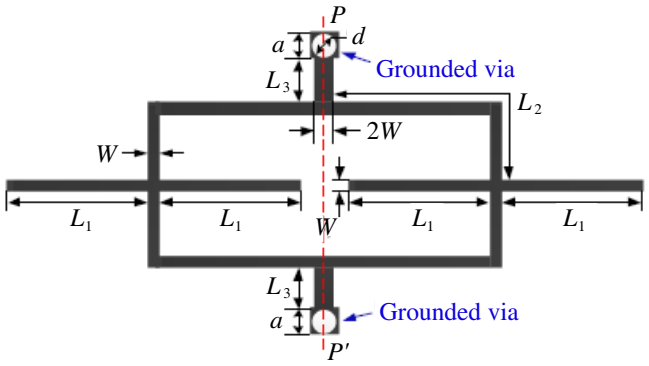

Figure 1. Structure of the proposed quad-mode stub-loaded ring resonator.

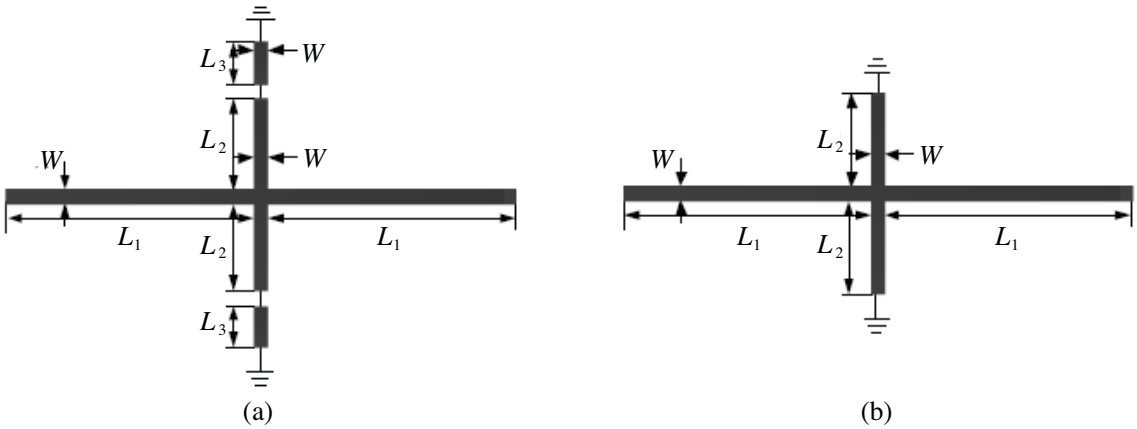

Figure 2. (a) Even-mode equivalent circuit of the quad-mode resonator and (b) odd-mode equivalent circuit of the quad-mode resonator.

The even- and odd-mode equivalent circuits are still symmetrical, so the even-odd-mode method is applied once again. Figures 3(a) and 3(b) show the even- and odd-mode equivalent circuits of Figure 2(a). Figures 3(c) and 3(d) show the even- and odd-mode equivalent circuits of Figure 2(b). Then, four modes named mode e_1, e_2, o_1, and o_2 are obtained. Each equivalent circuit of these four modes is a $\lambda/4$ resonator. The fundamental resonance frequencies of them are defined as f_{e1}, f_{e2}, f_{o1}

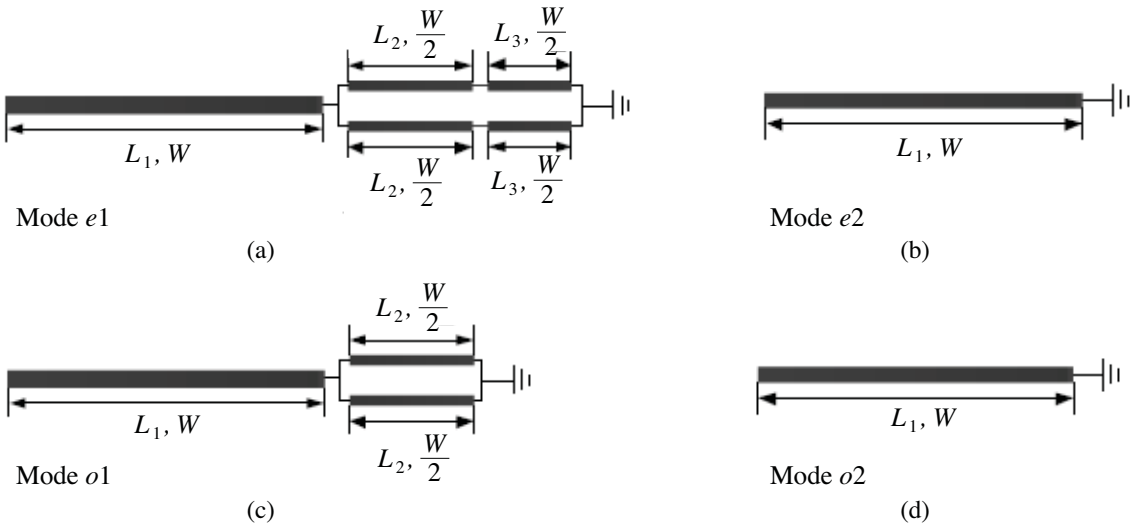

Figure 3. (a) Even-mode equivalent circuit of Figure 2(a), (b) odd-mode equivalent circuit of Figure 2(a), (c) even-mode equivalent circuit of Figure 2(b) and (d) odd-mode equivalent circuit of Figure 2(b).

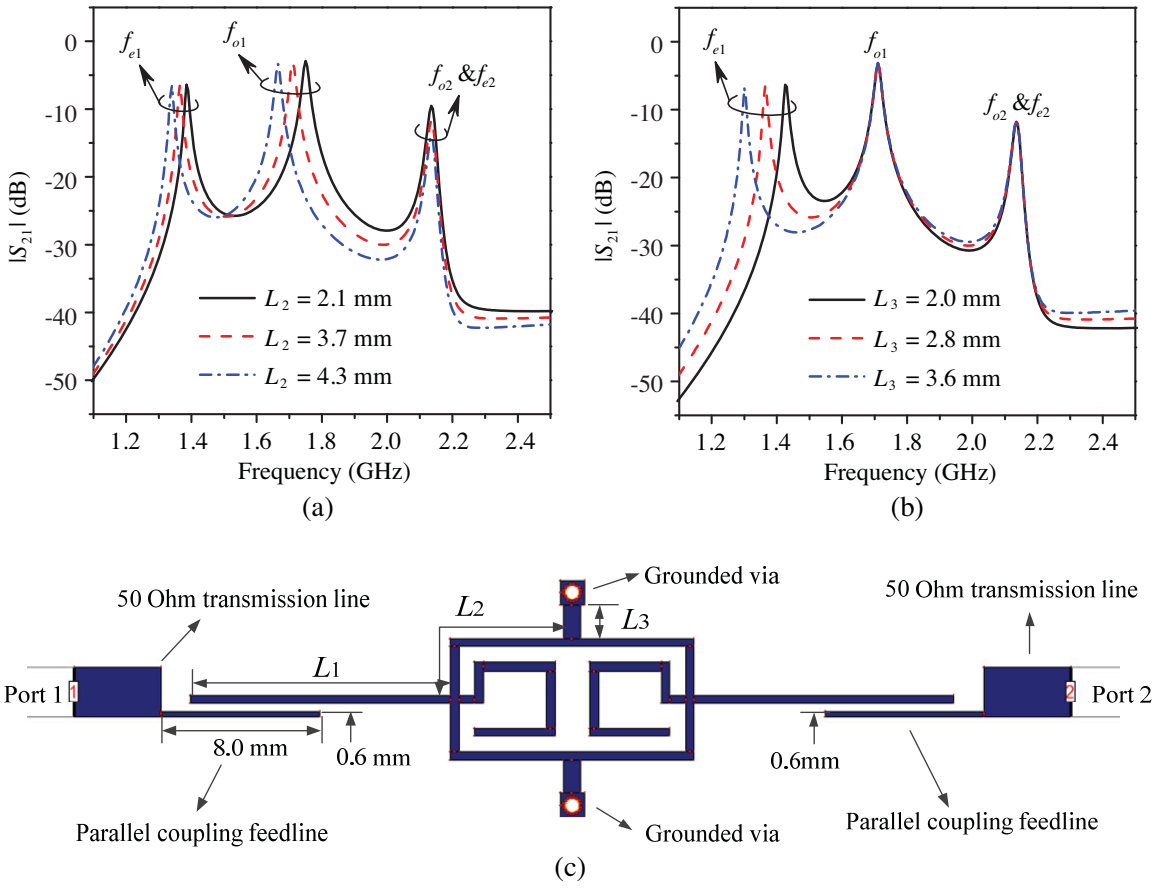

Figure 4. (a) Simulated S_{21} with varied L_2, (b) simulated S_{21} with varied L_3 and (c) PCB layout for computation of S_{21} under weak coupling.

and f_{o2}, with the relationship of $f_{e1} < f_{o1} < f_{e2} = f_{o2}$, and these four frequencies can be expressed in an explicit manner as follows:

$$f_{e1} = \frac{c}{4(L_1 + L_2 + L_3)\sqrt{\varepsilon_{eff}}} \tag{1}$$

$$f_{e2} = \frac{c}{4L_1\sqrt{\varepsilon_{eff}}} \tag{2}$$

$$f_{o1} = \frac{c}{4(L_1 + L_2)\sqrt{\varepsilon_{eff}}} \tag{3}$$

$$f_{o2} = \frac{c}{4L_1\sqrt{\varepsilon_{eff}}} \tag{4}$$

where c is the speed of the light in free space, and ε_{eff} denotes the effective dielectric constant of the substrate.

The simulated S_{21} of the resonator against L_2 and L_3 under weak external coupling are described in Figures 4(a) and 4(b), respectively. The PCB layout in IE3d software for computation of S_{21} is illustrated in Figure 4(c), the length of the parallel coupling feedline is set as 8.0 mm and the gap between the feedline and the stub of the resonator is set as 0.6 mm. Thus, the feedlines provide weak external coupling for the resonator, which is in favor of studying its resonance characteristics. As it is shown in Figure 4(a), the variation of L_2 changes f_{e1} and f_{o1}, while f_{e2} and f_{o2} keep constant. As shown in Figure 4(b), L_3 only relates to f_{e1}, while there is no influence on other frequencies. The same conclusions can be drawn from (1)–(4).

3. FILTER DESIGN, FABRICATION AND MEASUREMENT

In the above section, the resonance characteristics of the proposed quad-mode resonator are theoretically analyzed. Using this, two dual-band BPFs based on the quad-mode resonator will be designed in this section. To design dual-band BPFs based on the proposed quad-mode resonator, the two identical resonance frequencies f_{e2} and f_{o2} should be separated from each other to form the passband effect. In the design, two stubs are folded inward to introduce stub-stub coupling. The comparison of S_{21} with and without stub-stub coupling are illustrated in Figure 5. It can be seen that the two identical frequencies f_{e2} and f_{o2} are split, and two TZs are generated. The four modes are separated into two groups by TZs, so that there are two modes in each passband. Modes e_1, and o_1 form the lower passband, modes e_2, and o_2 form the upper one. The schematics of stub-stub coupling are showing in Figure 7 and Figure 8. The coupling strength can be freely controlled by the changing the gap between the two folded stubs.

In the design of dual-band filters, the distance between the two passbands and the range of the second passband should be chosen rationally. As shown in Figure 6, the first harmonic frequencies

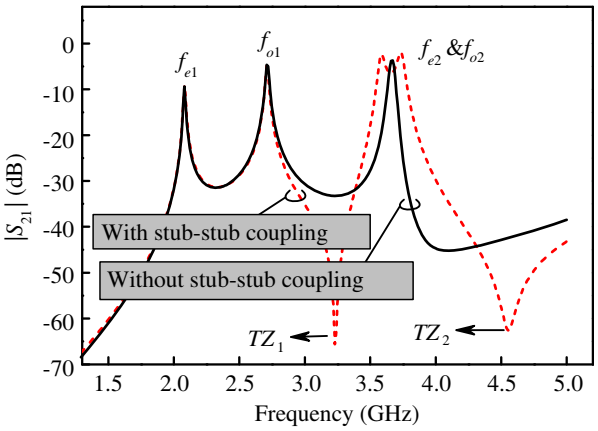

Figure 5. Simulated S_{21} with and without stub-stub coupling.

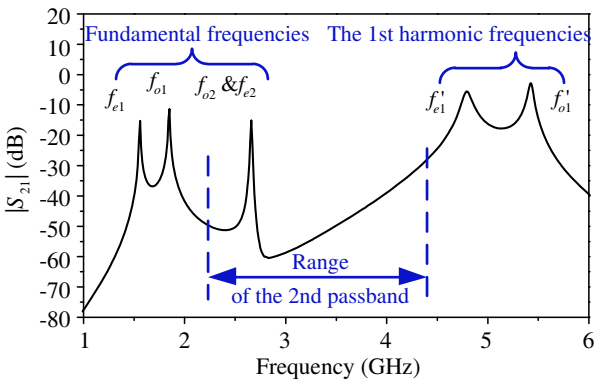

Figure 6. Limitations of the passband frequencies.

are approximately three times the fundamental ones, and the center frequency of the second passband should be less than them. Considering the structure of the resonator, there are two open stubs in the square ring, and for the purpose of eliminating the undesirable mutual coupling between transmission lines segments, the square ring should be large enough (i.e., the parameter L_2 should be great enough). Experiments and simulation show that the center frequency of the second passband should be greater than 1.3 times and less than 2.8 times the center frequency of the first passband. Through the analysis, both the two passbands center frequencies and bandwidths are independently controllable by tuning the corresponding parameters. The center frequency of the first passband can be controlled by L_2, and the center frequency of the second passband can be controlled by L_1. The bandwidths of the two passbands can be tuned by changing the in-band coupling coefficients of the two passbands. The in-band coupling coefficient of the first and the second passband are defined as $K_1 = |f_{e1}^2 - f_{o1}^2|/(f_{e1}^2 + f_{o1}^2)$ and $K_2 = |f_{e2}^2 - f_{o2}^2|/(f_{e2}^2 + f_{o2}^2)$ respectively. It can be observed from Figure 4(b) that f_{e1} shifts down with L_3 increased, while other frequencies keep constant. So the coupling coefficient K_1 will increase when L_3 increases, while there is no influence on K_2. From Figure 5, it can be observed that f_{e2} and f_{o2} are separated when stub-stub coupling is introduced, while f_{e1} and f_{o1} keep constant. So K_2 will increase when the strength of stub-stub coupling increases (i.e., decrease of the gap between the two folded stubs), while there is no influence on K_1. Therefore, the bandwidth of the first passband can be controlled by tuning the parameter L_3, the bandwidth of the second passband can be controlled by changing the the gap between the two folded stubs, and they can be tuned independently. Two dual-band BPFs working at 1.5/2.4 GHz and 1.5/3.5 GHz were then designed on the substrate with a relative dielectric of 2.45 and thickness of 1.0 mm.

In the design of the second filter, the hook-shape feed lines and source-load coupling are designed to produce two extra TZs between the two passbands, and high selectivity is achieved. Simulation and optimization were carried out by IE3d. Figure 7 and Figure 8 show the layout of the two filters. The optimized dimensions of filter 1 are determined as follows (all in mm): $L_1 = 8.3$, $L_2 = 10.5$, $L_3 = 12.1$, $L_4 = 4.9$, $L_5 = 7.5$, $L_6 = 2.5$, $L_7 = 3.5$, $L_8 = 4.3$, $L_9 = 2.0$, $L_{10} = 2.7$, $L_{f1} = 12.2$, $L_{f2} = 10.0$, $L_{f3} = 8.8$, $L_{f4} = 0.8$, $W = 0.5$, $W_f = 0.3$, $g_1 = 0.3$, $g_2 = 0.2$. The optimized dimensions of filter 2 are determined as follows (all in mm): $L_1 = 3.3$, $L_2 = 10.3$, $L_3 = 1.5$, $L_4 = 23.1$, $L_5 = 2.65$, $L_6 = 5.4$, $L_7 = 1.5$, $L_8 = 2.65$, $L_9 = 2.0$, $L_{10} = 8.15$, $L_{11} = 1.5$, $L_{12} = 3.9$, $L_{13} = 1.5$, $L_{14} = 2.5$, $L_{15} = 1.15$, $L_{16} = 3.1$, $L_{17} = 1.5$, $L_{f1} = 12.3$, $L_{f2} = 9.2$, $L_{f3} = 7.1$, $h = 1.2$, $W = 0.5$, $W_f = 0.3$, $g_1 = 0.2$, $g_2 = 0.9$, $g_3 = 0.3$, $g_4 = 0.5$. The overall circuit sizes of the two filters are $0.15\lambda_g \times 0.12\lambda_g$ and $0.13\lambda_g \times 0.11\lambda_g$, where λ_g is the guided wavelength at the center frequencies of the first passband (1.5 GHz). In the optimization, the relationships between the physical parameters and the performance were studied by coarse tuning, and the ranges of the physical parameters were determined. Based on this, reasonable convergence error was set. Then, the parameters were fine-tuned until the error is less than what was set.

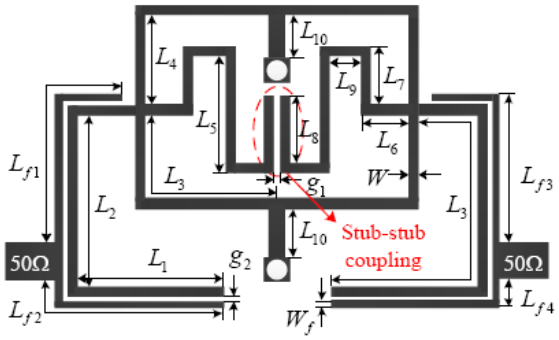

Figure 7. Layout of the proposed dual-band BPF 1.

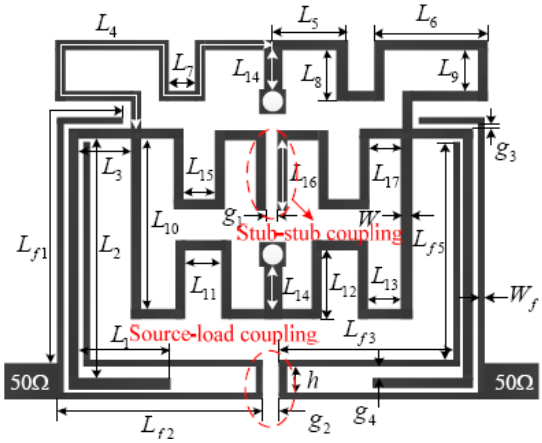

Figure 8. Layout of the proposed dual-band BPF 2.

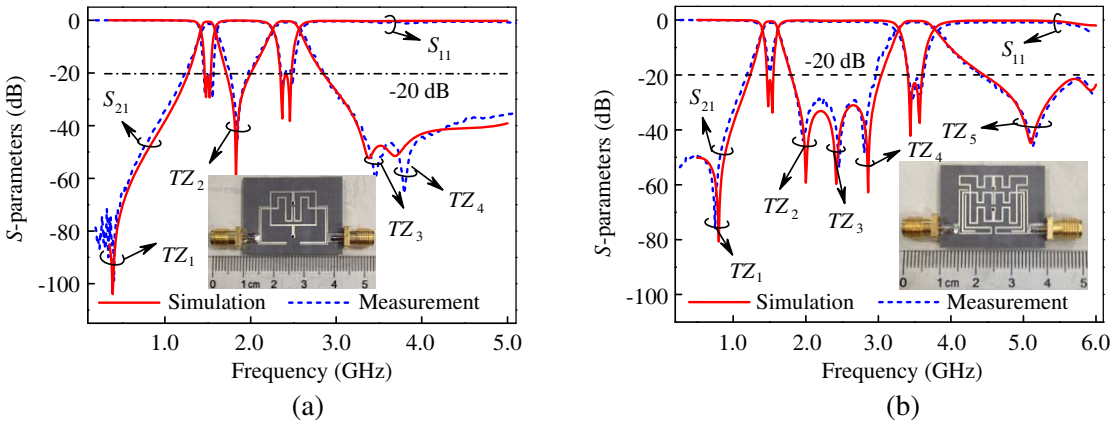

Figure 9. Measured and simulated results of the dual-band BPFs. (a) Measured and simulated results of BPF 1 and (b) measured and simulated results of BPF 2.

The designed filters were then fabricated and measured, and the measurement was performed on an Agilent 8917ES network analyser. The simulated and measured results are compared in Figure 9, along with the photographs of the fabricated filters. The measured passbands of the two filters, which are centred at 1.51/2.4 GHz and 1.5/3.52 GHz, have insertion losses less than 1.2/0.68 dB and 0.92/0.81 dB, the 3 dB fractional bandwidths are 9.5/13.1% and 12.5/14.6%, respectively. For filter 1, within the passbands, return losses better than 18.6 dB are obtained. The stopband is extended up to 5.1 GHz with rejection greater than 20 dB. The filter has four TZs located at 0.4, 1.84, 3.45 and 3.79 GHz. For filter 2, within the passbands, return losses better than 19.0 dB are obtained. The stopband is extended up to 6.1 GHz with rejection greater than 20 dB. The filter has five TZs located at 0.75, 1.97, 2.45, 2.80 and 5.13 GHz. Finally, Table 1 is provided to compare the second dual-band filter in this paper with those in [1, 2, 4, 15] in terms of a few key parameters. It can be observed that the proposed filter in this paper occupies smaller size, exhibits better performance in passband and has more TZs.

Table 1. Performance comparison between this work and filters in other papers.

Reference	Center frequencies (GHz)	$\|S_{21}\|$ (dB)	$\|S_{11}\|$ (dB)	Number of TZs	Circuit size ($\lambda_g \times \lambda_g$)
[1]	2.45/5.25	1.7/1.5	14/20.1	3	0.14×0.104
[2]	1.84/2.65	0.43/0.65	13.4/15.5	4	0.17×0.21
[4]	1.6/2.45	1.46/1.16	12/12	2	0.22×0.21
[15]	2.4/5.16	0.6/1.4	19 /12	4	0.46×0.42
This work	1.5/3.52	1.1/0.84	19.0/21	5	0.13×0.11

4. CONCLUSIONS

In this paper, a novel quad-mode resonator is proposed. Each mode equivalent circuit is a $\lambda/4$ resonator. So the resonator has a compact size and relatively higher harmonics. Based on the proposed resonator, two dual-band BPFs operating at 1.5/2.4 GHz and 1.5/3.5 GHz are designed. In the design of the second filter, hook-shape feed lines and source-load coupling are introduced to generate extra TZs, which effectively improve the isolation level between passbands. The designed filters exhibit very good in-band performance and high selectivity. Moreover, their frequencies and bandwidths can be individually controlled. Therefore, the proposed filters will be attractive in multi-band wireless communication systems.

ACKNOWLEDGMENT

This work was supported by the National Natural Science Foundation of China (NSFC) under Project No. 61271017 and No. 61301069, and the Fundamental Research Funds for the Central Universities No. JB140226.

REFERENCES

1. Zhou, M., X. Tang, and F. Xiao, "Compact dual band bandpass filter using novel E-type resonators with controllable bandwidths," *IEEE Microw. Wireless Compon. Lett.*, Vol. 18, No. 12, 779–781, Dec. 2008.
2. Yang, S., L. Lin, J.-Z. Chen, K. Deng, and C.-H. Liang, "Design of compact dual-band bandpass filter using dual-mode stepped-impedance stub resonator," *Electronics Letters*, Vol. 50, No. 8, 611–613, Apr. 2014.
3. Sun, S.-J., T. Su, K. Deng, B. Wu, and C.-H. Liang, "Shorted-ended stepped-impedance dual-resonance resonator and its application to bandpass filters," *IEEE Trans. Microw. Theory Tech.*, Vol. 61, No. 9, 3209–3215, Sep. 2013.
4. Zhang, X. Y., C.-H. Chan, Q. Xue, and B.-J. Hu, "Dual-band bandpass filter with controllable bandwidths using two coupling paths," *IEEE Microw. Wireless Compon. Lett.*, Vol. 20, No. 11, 616–618, Nov. 2010.
5. Kuo, J.-T. and S.-W. Lai, "New dual-band bandpass filter with wide upper rejection band," *Progress In Electromagnetics Research*, Vol. 123, 371–384, 2012.
6. Zhang, X. Y., J.-X. Chen, Q. Xue, and S.-M. Li, "Dual-band bandpass filters using stub-loaded resonators," *IEEE Microw. Wireless Compon. Lett.*, Vol. 17, No. 8, 583–585, Aug. 2007.
7. Ma, D., Z. Y. Xiao, L. Xiang, X. Wu, C. Huang, and X. Kuo, "Compact dual-band bandpass filter using folded SIR with two stubs for WLAN," *Progress In Electromagnetics Research*, Vol. 117, 357–364, 2011.
8. Kuo, J.-T., S.-C. Tang, and S.-H. Lin, "Quasi-elliptic function bandpass filter with upper stopband extension and high rejection level using cross-coupled stepped-impedance resonators," *Progress In Electromagnetics Research*, Vol. 114, 395–405, 2011.
9. Chu, Q. X. and F. C. Chen, "A compact dual-band bandpass filter using meandering stepped impedance resonators," *IEEE Microw. Wireless Compon. Lett.*, Vol. 18, No. 5, 320–322, May 2008.
10. Yao, Z., C. Wang, and N. Y. Kim, "A Compact dual-mode dual-band bandpass filter using stepped-impedance open-loop resonators and center-loaded resonators," *Microw. Opt. Technol. Lett.*, Vol. 55, No. 12, 3000–3005, Dec. 2013.
11. Sun, S.-J., T. Su, K. Deng, B. Wu, and C.-H. Liang, "Compact microstrip dual-band bandpass filter using a novel stub-loaded quad-mode resonator," *IEEE Microw. Wireless Compon. Lett.*, Vol. 23, No. 9, 465–467, Nov. 2013.
12. Jiang, W., L. Zhou, A.-M. Gao, W. Shen, W.-Y. Yin, and J.-F. Mao, "Compact dual-mode dual-band balun filter using double-sided parallel-strip line," *Electronics Letters*, Vol. 48, No. 21, 1351–1352, Oct. 2012.
13. Fu, S., B. Wu, J. Chen, S.-J. Sun, and C. H. Liang, "Novel second-order dual-mode dual-band filters using capacitance loaded square loop resonator," *IEEE Trans. Microw. Theory Tech.*, Vol. 60, No. 3, 477–483, Mar. 2012.
14. Sung, Y., "Dual-mode dual-band filter with band notch structures," *IEEE Microw. Wireless Compon. Lett.*, Vol. 20, No. 2, 73–75, Feb. 2010.
15. Li, Y.-C., H. Wong, and Q. Xue, "Dual-mode dual-band bandpass filter based on a stub-loaded patch resonator," *IEEE Microw. Wireless Compon. Lett.*, Vol. 21, No. 10, 525–527, Oct. 2011.
16. Chiou, Y.-C., P.-S. Yang, J.-T. Kuo, and C.-Y. Wu, "Transmission zero design graph for dual-mode dual-band filter with periodic stepped-impedance ring resonator," *Progress In Electromagnetics Research*, Vol. 108, 23–36, 2010.

17. Zhao, L.-P., D. Li, Z.-X. Chen, and C.-H. Liang, "Novel design of dual-mode dual-band bandpass filter with triangular resonators," *Progress In Electromagnetics Research*, Vol. 77, 417–424, 2007.
18. Luo, S. and L. Zhu, "A novel dual-mode dual-band bandpass filter based on a single ring resonator," *IEEE Microw. Wireless Compon. Lett.*, Vol. 19, No. 8, 497–499, Aug. 2009.
19. Belyaev, B. A., A. M. Serzhantov, and V. V. Tyurnev, "A miniature dual-band filter based on microstrip dual-mode resonators," *Technical Physics Letters*, Vol. 38, No. 9, 839–842, 2012.
20. Belyaev, B. A., A. M. Serzhantov, and V. V. Tyurnev, "A dual-mode split microstrip resonator and its applications in frequency selective devices," *Microw. Opt. Technol. Lett.*, Vol. 55, No. 9, 2186–2190, 2013.
21. Sun, S., "A dual-band bandpass filter using a single dual-mode ring resonator," *IEEE Microw. Wireless Compon. Lett.*, Vol. 21, No. 6, 298–300, Jun. 2011.